Instrument: **SP1 Cooperation**

Thematic Priority: **Priority Area 1.1.6.3 "Global Change and Ecosystems"**

FP7 Collaborative Project – Grant Agreement 212492

CLARIS LPB
A Europe-South America Network for Climate Change Assessment and Impact Studies in La Plata Basin

DELIVERABLES

D9.14: Prediction of climate change scenarios effects on navigation partner, dredging needs and bank stability in the Lower Paraná River

Due date of deliverable: Month 42

Start date of project: **01/10/2008** Duration: 4 **years**

Organisation name of lead contractor for this deliverable: University of Bologna

Deliverable No	Deliverable title	WP	Lead beneficiary	Estimated indicative person-months (permanent staff)	Nature	Dissemination level	Delivery date
D9.14	Prediction of climate change scenarios effects on navigation pattern, dredging needs and bank stability in the Lower Paraná River	9	P16-INA	***	O	CO	42

Massimo Guerrero[(1)], *Letizia Pastorello*[(1)]
Angel N. Menéndez[(2)], *Mariano Re*[(2)], *Leandro D. Kazimierski*[(2)]

[(1)]*Hydraulic Laboratory, University of Bologna, Bologna, Italy*
[(2)]*Hydraulic Laboratory, National Institute for Water (INA), Ezeiza, Argentina*

Introduction

Concerning the climate of La Plata Basin the XX century can be subdivided into three periods as reported by Garcia and Vargas, 1998, Garcia et al., 2002 and Jaime and Menéndez (2002), with a dry period of 40 years in the middle and wet periods at starting and closure of the century. In particular the precipitations had the same behaviour in the upper and lower basin therefore giving rise to the same streamflow tendency changes within the century. A near 30 year long period can be argued in the stream flow variability (i.e. interdecadal variability) that can be correlated to climate indices (Maciel et *al.*, 2010). Furthermore some evidences exist that a certain increment of discharge starting from 1970-1971 was due to land use change on the Brazilian area of the basin, began in 1968 (Garcia et *al.*, 2002). That increment differently summed with increased rainfall increment depending on La Plata Basin areas. In particular Doyle and Barros (2010) show as the runoff increasing was caused by land use change in the north, by climate variability in the south and by both in the middle part of the basin. The same authors show as extreme events recurrence is not strongly correlated with interdecadal variability at Corrientes (northern part of Paraná River) meanwhile it appears better correlated to hydrology-climate variability for the Uruguay River at Paso de los Libres. This occurrence bears out the evidence that streamflow increasing at Lower Paraná was mainly related to climate variability.

Amsler et al. (2005) quantitatively analyzed as the streamflow interdecadal variability affected the channel morphology of Paraná River in its middle reach during XX century, meanwhile Castro et *al.* (2007), carried out a similar study for a 50 km long reach at very beginning of Lower Paraná between Puerto San Martin and Alver (nearby Rosario City). The former study clearly correlates climate interdecadal variability to effective discharge (i.e. the discharge value most effective modifying the

morphology) variability and as a consequence to river morphological changes. In particular the dry midst of the century (1930-1970) was characterized by low effective discharge that promoted a decrease in width, braided index, thalweg sinuosity, width to depth ratio and channel volume, vice versa for the century begin and end. In other words, for Middle Paraná, the dry period accomplished to reduce sediment transport and river channel planimetric dimensions while wet periods, on the contrary, increased sediment transport and enlarged river channel giving rise to islands formation within it. The Lower Paraná morphodynamics is not straightforward correlated to hydrological variability as much as the Middle Paraná. In particular, historical cartography of the reach between San Martin and Rosario bears out a continuously and progressive oversimplification of the river channel planimetric morphology toward a lower width to depth ratio. The last part of the century, since 1970, not recovering the extremely braided morphology that characterized the century begin, on the contrary exacerbating the midst century morphodynamics processes. This occurrence is not easy justified by hydrology interdecadal variability therefore the authors found additional reasons in the alluvial plane morphology that starting from San Martin up to the La Plata River strongly enlarge and decrease in slope. This morphology constrains together with increased effective discharge, during the last part of the century, would has produced sediment deposition at secondary reaches and therefore the streamflow gathering in a single straight and deep reach. As a matter of fact the authors report evidences on decreased water slope at effective discharge that is correlated to sediment deposition increasing.

The Lower Paraná reach between Rosario and San Martin is also a strategic area for inner navigation, as part of the navigation route ‘Santa Fe to the Ocean’ (Figure 1). Besides the morphology singularities of the areas as the bifurcations and junction (recognized as key features for river channel morphology development), sedimentation on the navigation channel drives our attention.

Figure 1. 'Santa Fe to the Ocean' navigation route.

In Lower Paraná River, the navigation route for oceanic vessels is the most important maritime export route in Argentina. This navigable waterway concentrates 80% of local agricultural exports, the highest siderurgical traffic in the country, and gathers the transport of general fluvial and vessel loads that originate in or are destined to the Buenos Aires port. This route is naturally navigable for most of its length (approximately 550 km), the lack of depth problems occurs in localized areas, which constitute the so-called critical stretches (pasos críticos), on which are dredged artificial navigation channels. The natural tendency sediment deposition in these channels requires regular and systematic maintenance dredging. The annual volume of maintenance dredging is a vital indicator to determine the economic feasibility of ensuring a certain depth.

Climate Change produces a series of consequences for the river navigation. Changes in precipitation at the basin alter the occurrence of extreme hydrological conditions and, indirectly, alter the navigability (PIANC, 2008). Climate Change can also force changes in river morphology (by variations in the processes of erosion and sedimentation), in vessels maneuverability and in the operational efficiency of navigation structures (Hawkes et al., 2010). Background in assessing Climate Change impacts on navigation have focused primarily on the determination of variations in water levels due to changes in basin hydrological variables (Sung et al., 2006; de Wit et al., 2007; Millerd, 2011).

In this framework, present contribution has two approaches: one is aimed to clarify the Lower Paraná general morphodynamics during XX century in the light of mentioned interdecadal variability, morphological constrains and land use change; and the other to assess sedimentation in navigation channels developing a methodology in a particular critical stretch.

For first case we applied two numerical models to simulates river hydro-morphodynamics: HEC-RAS (U.S. Army Corps of Engineers, 2008), a 1D model to reproduce effective discharge, water levels and bed slopes changes in the whole Paraná river from Corrientes to Villa Constitución (865 km); and MIKE 21C (DHI Water and Environment, 2002), a 2D model that was applied in a 24 km long reach of the Lower Paraná (from Puerto San Martin to Rosario-Victoria bridge, studied by Castro et al. 2007, Figure 2) to simulate local deposition and therefore river channel tendency towards braided or meandering single channel configuration. The 1D model was used to predict the bed level change of the Paraná River for the XXI century to be compared with the simulation of the past hydrology (XX century) and to supplied boundary conditions in terms of water levels, volume and sediment discharges for 2D model morphodynamic simulations. The 2D model was applied to make sensitive analyses on sediment transport deviation due to secondary flows (along the 24 km reach and including a 2 km wide portion of the alluvial plane) with the aim to reproduce the channel morphology changes that were observed in the period 1954-1976. Therefore the period 2010-2040 was simulated assuming a reliable configuration for

the downstream outlet morphology (i.e., bifurcated thread) and a water depth-bed roughness law is introduced to account of vegetation at submerged islands and alluvial plane.

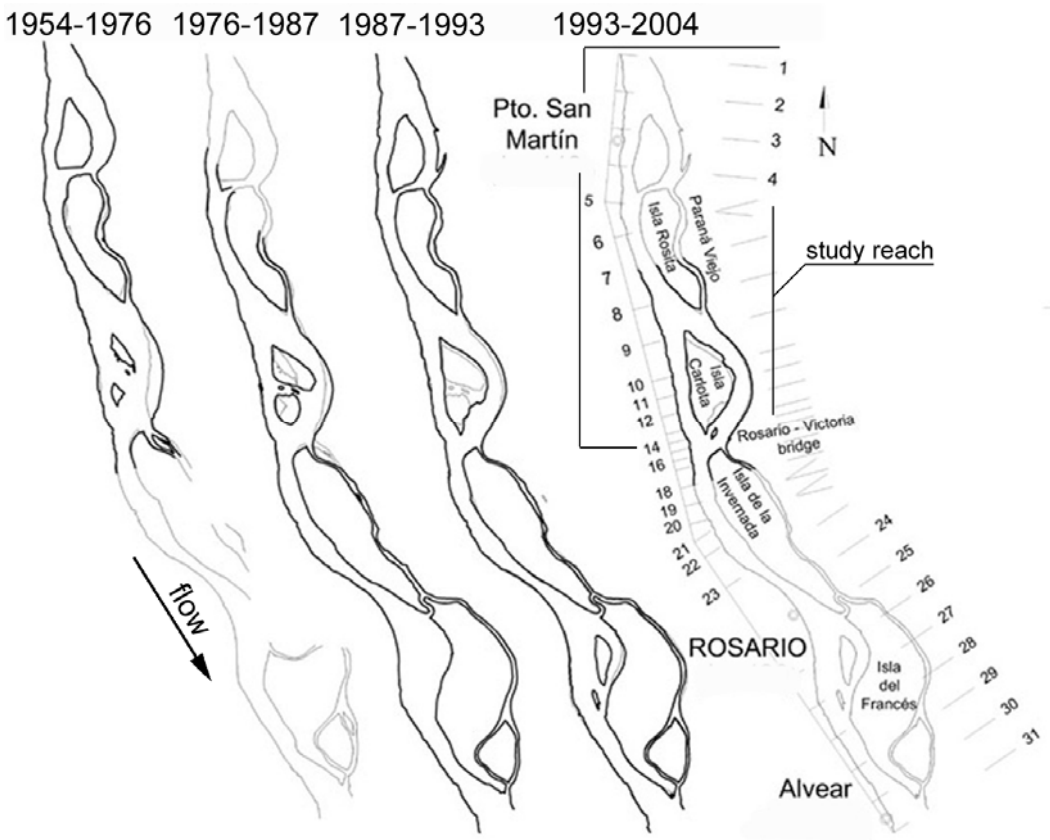

Figure 2 Margin comparisons at Lower Paraná reach in the XX century.

For the second case, a numerical modeling methodology for sedimentation in navigation channels is used to evaluate effects of Climate Change, through consideration of potential changes in the river discharge. This methodology, which is explained in detail, is illustrated through its application to a critical stretch of the Lower Parana River, validating its results with maintenance dredging data. It is shown that, keeping the present dredging elevations, the sedimentation volume would increase with the increment in discharge, and vice versa, with relative rates of change significantly larger than that of the discharge. If, on the contrary, the dredging elevations were adjusted to new reference levels, the trend would be the opposite, with relative rates of change only moderately larger than that of the discharge, in absolute

value. Establish the probably evolution of maintenance dredging in the context of Climate Change is thus an exercise of great importance for management. As illustration of the methodology an analysis section of the Parana River was chosen, corresponding to Paso Borghi, near the city of Rosario, which is one of the critical stretches most relevant.

Lower Paraná general morphodynamics

1D model of Paraná River

Aim of the 1D simulation is to validate a methodology to assess the impact of solid and liquid discharge regime change on river bed slope and to provide flow, sediment discharges and level time series to be applied as boundary conditions in the 2D model.

The calibration of the model was already presented in the D9.13.

Figure 3 shows the modeled Paraná reach from Corrientes to Villa Constituciòn and four significant cross-sections.

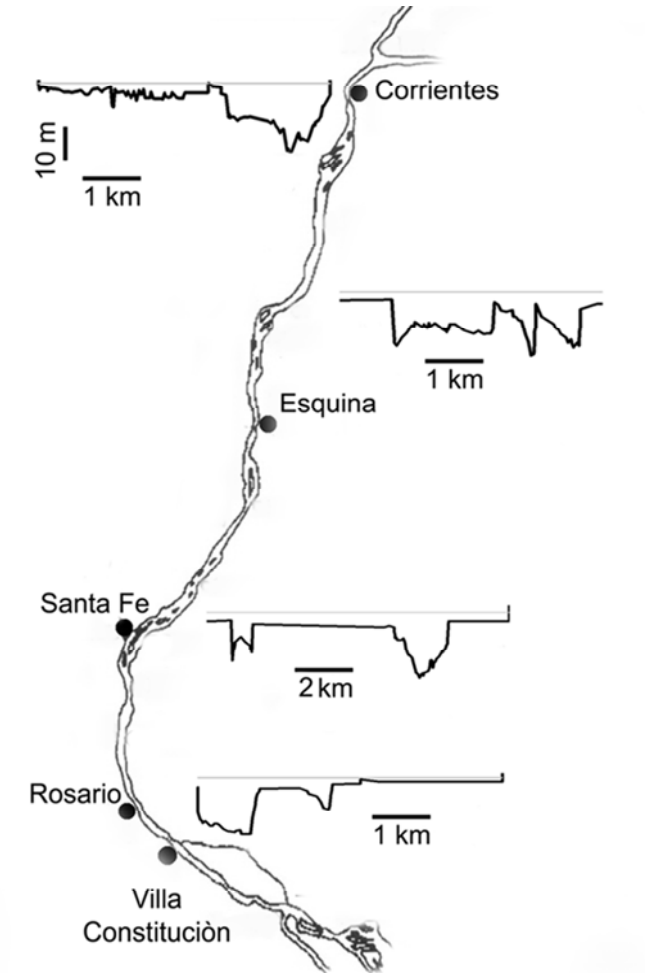

Figure 3. 1D modeled Paraná reach.

Future scenarios

Two continuous time-series of flow-discharge are simulated predicting the XXI century hydrology. The series resulted from the hydrological distributed model VIC that was applied to La Plata Basin by the University of Buenos Aires, assuming as input the results of the Regional Climate Models (RCM) PROMES by the University of Castilla and La Mancha (Spain) and RCA by the Swedish Meteorological and Hydrological Institute, respectively. The RCMs were forced with boundary conditions obtained from HadCM3 and ECHAM5 Global Climate Models (GCM), respectively, and in both cases the A1B scenario for CO2 emission was considered. Details about the hydrological and climate models can be found in Fernandes et al. (2011) and Solman et al. (2011) respectively. The effective discharge results 15'000 m^3/s for the past century and increases of 50% for the scenario time-series, therefore changing to 23'000 m^3/s, as shown in Figure 4 where 20, equal representative, classes of flow discharge are reported against conveyed sediment volume per year.

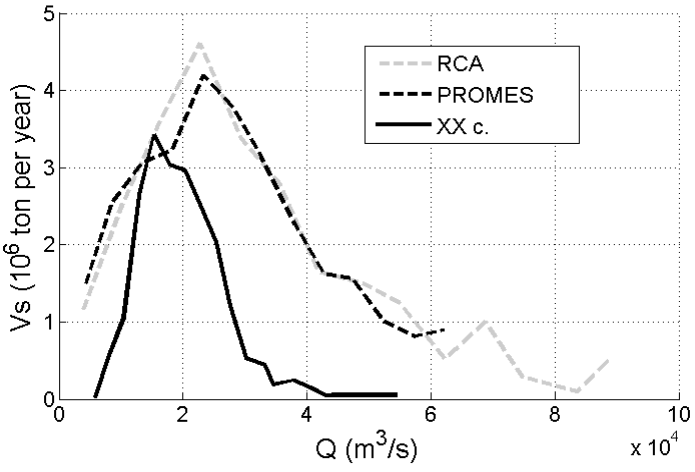

Figure 4. Classes of Flow discharge Q and its corresponding sediment volume per year, in the period XX century and for the PROMES and RCA time-series

The spectral analyses of the XX century and forecasted time-series of flow-discharge are compared in Figure 4 at different frequency ranges. The amplitude of variability increases passing from the past data

to the projections and among almost the entire frequency ranges. In particular, the RCA model generates the largest amplitudes albeit the corresponding average discharge is lower than the PROMES time-series mean value as it is also reflected in the effective discharges. Therefore the RCA simulates a larger variability over a lower mean value; the RCA and PROMES standard deviations being 15'400 m^3/s and 15'000 m^3/s respectively, and the corresponding mean 19'000 m^3/s and 20'300 m^3/s. Significant amplitudes appear in Figure 5a around 4-6 months and 1 year, corresponding to 2-3 and 1 as frequencies, for the modeled and past time-series, meanwhile at smaller frequencies, i.e., larger time periods, 5-10 and 20 years variabilities can be argued (Figure 5b) both for simulated and past time-series. The longest period variability (10-20 years) is particularly amplified by the RCA model.

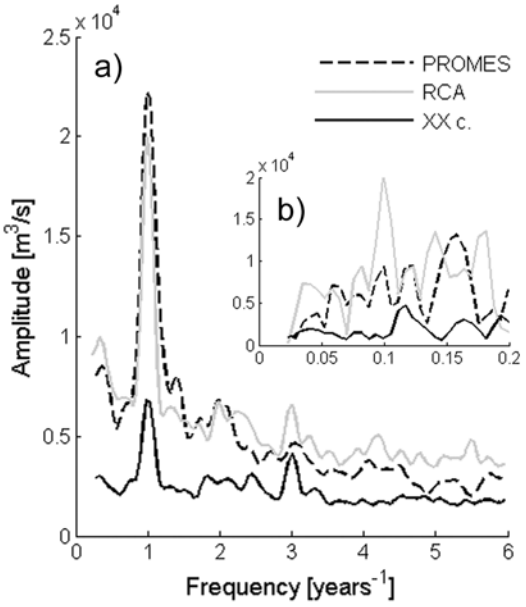

Figure 5. Spectral analyses of XX century and forecasted (PROMES and RCA XXI century projections) time-series of flow-discharge; high a) and low b) frequency ranges.

Figure 6 reports the simulated evolution of river morphology in terms of bed-level change for the past time-series and for the hydrological scenarios of the XXI century as inferred by means of RCA and PROMES. The model amplifies the bed-level changes along the river in reason of the increased hydrology maintaining almost everywhere the same aggradation or degradation tendencies as for the past

century. In particular the deposition at Lower Paraná around the 500 kilometer would be almost doubled meanwhile the more downstream part, nearby the Delta, results almost stable.

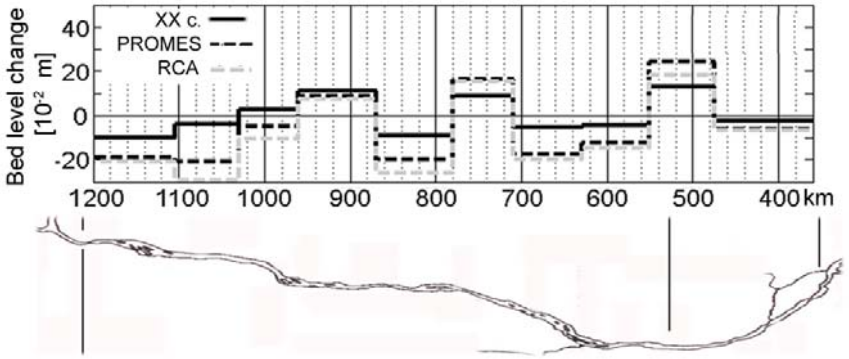

Figure 6. Bed-level change during the XX century (solid line) and the PROMES and RCA projections for the XXI century (dashed lines).

The resulting bed-level changes by considering PROMES and RCA projections are pretty near that occurrence bears out a low sensitivity of the river channel 1D morphology to different climate projections.

The 1D model also provides the boundary conditions for the 2D simulated calibration (1954-1976) and projection (2010-2040) periods in terms of average effective discharge Q_{eff} on ten years basis, corresponding duration d, water level h_{eff} and conveyed volume of sediments per year G_s. The water level h_{eff} is imposed at downstream boundary (Rosario-Victoria Bridge) of the 2D model. The simulated conveyed sediments, G_s, corresponds to the 60% of the entire sediment volume; the assessed average effective discharge, Q_{eff}, transporting the 60% of the entire sediment volume. Therefore the 2D simulations represent the most significant part of the 30 years hydrograph in terms of transported sediment volume and corresponding morphodynamics; the transported volumes are in fact negligible at low flow discharge or for short duration high flows (15% tails in Figure 4).

Tables 1 and 2 report the 2D modelled conditions for the calibration and for the projection scenarios respectively, in the latter case the last decade values are also reported.

Table 1. Effective discharge, corresponding water level, duration and conveyed volume of sediments to be applied as boundary conditions in the 2D model for the calibration period (1954-1976).

Period	Q_{eff} (m^3/s)	h_{eff} (m)	d (month)	G_s (mil ton /y)
1950-1960	18800	6.3	65	17
1960-1970	13700	4.6	77	15
1970-1980	16800	5.6	74	24

Table 2. Effective discharge, corresponding water level, duration and conveyed volume of sediments to be applied as boundary conditions in the 2D model for the projections (PROMES, *RCA*) period (2010-2040) and for the last decade.

Period	Q_{eff} (m^3/s)	h_{eff} (m)	d (month)	G_s (mil ton /y)
2000-2010	15100	5.0	64	19
2010-2020	*24600*	*8.2*	*61*	*32*
	22900	7.6	52	48
2020-2030	*24700*	*8.2*	*64*	*34*
	24500	8.2	65	23
2030-2040	*27100*	*9.0*	*50*	*42*
	24700	8.2	57	32

2D model of Lower Paraná case study

The 24 km long reach of Lower Paraná (**¡Error! No se encuentra el origen de la referencia.**2) was surveyed during three field campaigns in June 2009, August 2009 and November 2010, as reported in the D9.13.

The validation of the 2D numerical model MIKE21C by DHI was performed in three distinct phases: the bed roughness was calibrated within the shallow-water approach of the model, by the comparison of measured and computed depth maps and velocity vectors at surveyed cross-sections; then the sediment transport formula of Engelund and Hansen was verified on measured concentration (Guerrero et al., under review); finally, the long term morphodynamic simulations are carried out in order to reproduce the island Carlota formation process occurring in the period accounting of hydrodynamic and sediment transport former calibration results and of the historical cartography. These phases were already

described in the D9.13, while the extension of the carried out sensitivity analysis on 1954-1976 morphodynamics is herein presented.

Two future scenarios (2010-2040) were then simulated aiming to predict the effectiveness of the two climate projections (RCA and PROMES models derived) in modifying the river channel morphology. The resulting morphology was also compared to a 30 years period simulation result with a constant effective discharge (i.e., 2000-2010 value).

The morphodynamic simulations (calibration and projection periods) were carried out with a quasi-steady approach that is fitted for long-term simulation of river channel morphodynamics. The characterized 10 years intervals were assumed for boundary conditions aiming to capture the interdecadal variability of the hydrology time series and to filter out year and seasonal variability which negligibly affect the river channel morphology. The assumed morphological time step is 6 hours, while the boundary conditions were maintained fixed within the same decade. The hydraulic calculations were scaled in agreement to the applied hydrodynamic time step of 5 s, which is defined by numerical convergence requirement.

Morphodynamics calibration

The morphodynamic calibration was carried out on the 1954-1976 period, reproducing the Carlota island formation which took place within river cross-sections 9-14 in Figure 7. As can be seen in Figure 7, the Carlota sub-reach significantly changed during the XX century in a way that is representative of Lower Paraná morphodynamics. The Carlota Island was formed in the middle of the active part of the river as the consequence of a deposition process that took place at Lower Paraná.

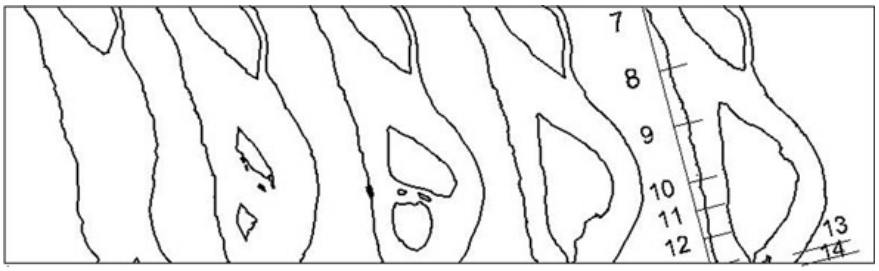

Figure 7. Margin development of Carlota Island (1954-1976-1987-1993-2004 from left to right).

As a matter of fact, due to its bed slope, the sediment transport capacity of Lower Paraná is lower than Middle Paraná capacity as it arises from 1D model. The deposition at Lower Paraná occurred among the whole XX century driving river channel from intricate braided morphology to a meandered-bifurcated configuration that is characterized by the sequence of well defined islands between a straight main channel and a secondary bended channel. That oversimplification was particularly intense during the second part of XX century, corresponding to a humid period driven by climate interdecadal oscillation (Amsler et al., 2005) that probably also intensified the unbalance between Lower and Upper Paraná sediment transport capacities. Figure 2 and Figure 7, more detailed for Carlota Island, show the margin collections from 1954 to 2004 that witnesses the described morphology change. In particular the Carlota island formation arose at cross-sections 9 to 14, between 1954-1976 period. That process was also characterized by the left margin displacement of 1.5 km within 1954-2004 and by the diversion of main flow from left bended to right straight channel. Castro et al. 2007 carried out a detailed morphology analysis of the whole reach of Figure 2, also reporting that the water volume and the averaged depth of main channel respectively changed from 9.5×10^6 m^3/km and 5.2 m to 10.1×10^6 m^3/km and 7.4 m within the period 1950-2005, for the 10 km that include the Carlota Island. The 1954 bathymetry was reconstructed starting from the survey bathymetry of 2009 and on the basis of historical margins in Figure 7, the mentioned literature data and the averaged level resulting from 1D model. The water volume and the depth as average over the Carlota island reach resulted equal to 9.1×10^6 m^3/km and 4.6 m respectively for 1954 and 15.5×10^6 m^3/km and 8.1 m for 2009.

The reconstructed bathymetry of 1954 was therefore forced with steady conditions at the boundaries as resulting from 1D model for the calibration period (Table 1).

The morphodynamic calibration consists of a sensitivity analysis that was performed on final morphology by modifying the sediment transport portion which is deviated from stream flow direction because of secondary flows and the transversal slope of the river bed. This analysis was already introduced in D9.13. The results on the extended grid (Figure 8), including the entire study reach and a 2 km wide portion of the alluvial plane, are herein reported. Three simulations were performed with an increasing influence of bed transversal slope in deviating sediment direction by means of the G coefficient (D9.13 and Guerrero et al. under review-b). Downstream of Victoria Bridge, the left reach was assumed as a dead reach (closed by sediment deposition) in order to simulate the left margin erosion that is observed in the margins historical series (Figure 2 and 7). Figure 8 shows the initial bathymetry and the final morphologies as resulting with different G values together with 1976 historical margins (black line). The observed morphological changes appear better simulated by a G value around 2-2.5, as a matter of fact for G=2.5 the bifurcation at Carlota Island upstream is represented, two well defined islands appear, in some way simulating 1976 island margins, and the main flow is clearly diverted from left arms to the straight right one as a consequence of the bar formation at left margin. The two thread configuration is not well represented for G equal to 1.5; while the median value of G gave rise to a reliable morphology with two main reaches and a third dead one ending at the location of the island formation. G=2 was finally selected for the following simulations.

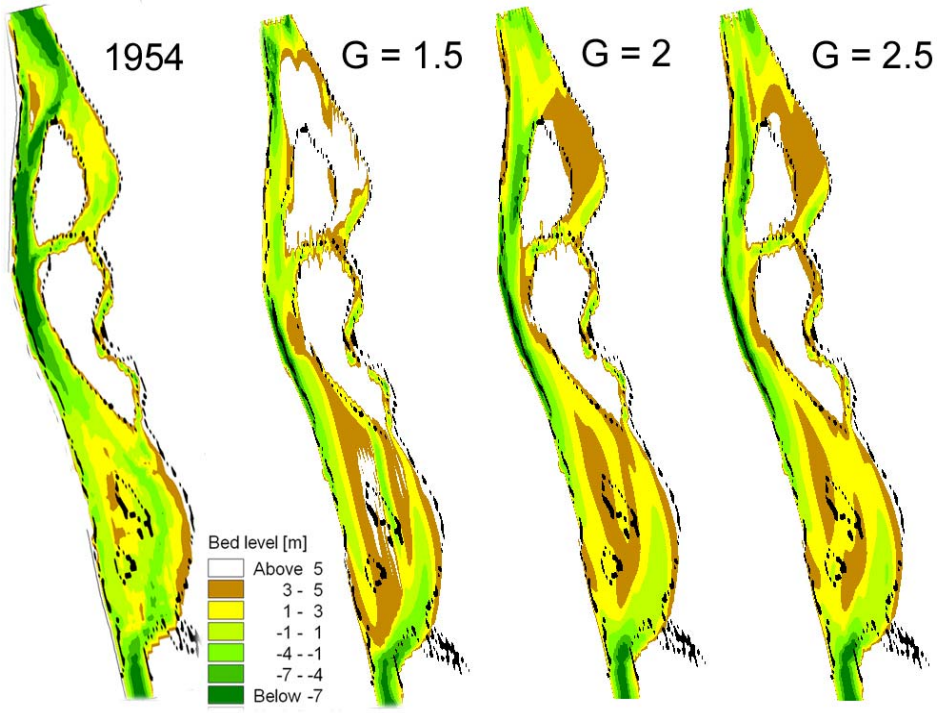

Figure 8. Comparison of 1976 historical margin (black line) to initial (1954) and resulting bed level maps from 2D model simulations of 1954-1976 period and for different transversal slope parameter (*G*) values.

Future scenarios

The calibrated model was applied to the bathymetric survey (2009) and with the hydrology-sediment transport conditions (Table 2) derived from PROMES and RCA forced 1D simulations. On the basis of the two scenarios increased discharge, a bifurcated morphology was assumed at the downstream boundary therefore reopening the left reach that was filled with sediment during the past century as it appears from historical margins sequence (Figure 2). Figure 9 shows the initial bathymetry (a) and the final morphology (c and d) as resulting for the two future time series and for the 30 years run with the last decade conditions (b). Notwithstanding the same steady morphologies were assumed at model boundaries, i.e. single and bifurcated threads at upstream and downstream boundaries respectively, very different morphologies resulted because of the future projections increased hydrology. In fact the 30 years simulation of the last decade conditions doesn't give rise to significant changes of river channel morphology, albeit a widespread deposition and the consequent thalweg reduction can be argued, while the two climate scenarios predict a dramatic change in the river channel morphology. In particular the upstream island is completely eroded, the two left reaches are almost merged by means of the secondary

reach activated at left margin, the straight right reach is significantly eroded, all in all the water and sediment conductivity of the river is significantly increased.

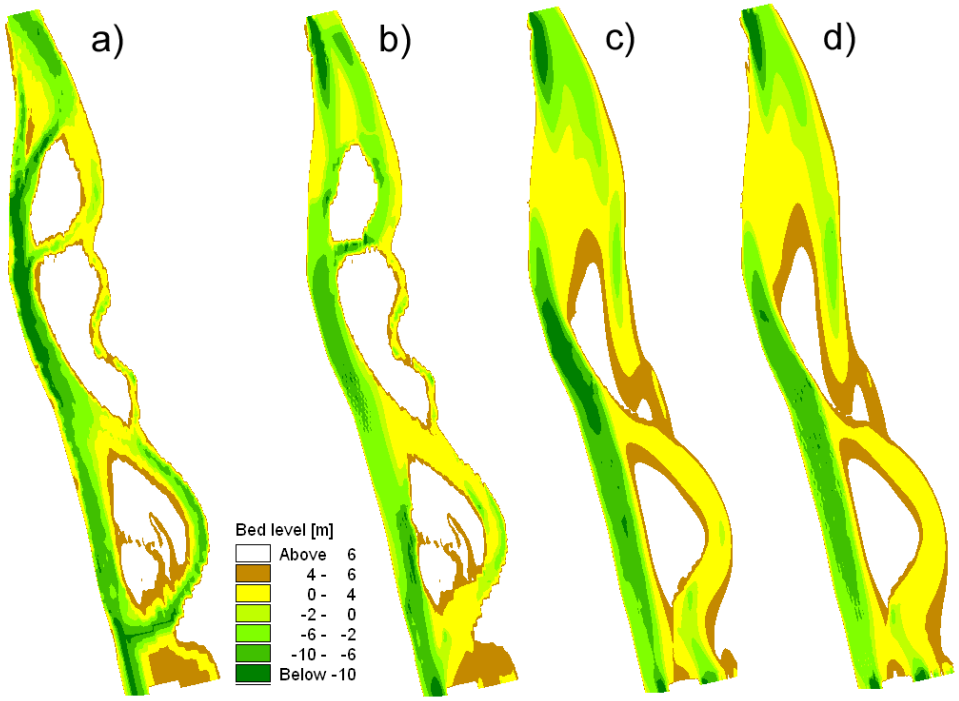

Figure 9. Initial (a) and final bed level maps from 2D model simulations of 2010-2040 period for last decade (b), RCA (c) and PROMES (d) scenarios.

Concerning the bed-roughness, some evidences were derived from 2009 and 2011 surveys at the study reach. In fact, in Guerrero et *al.* (under review) the values of 56 and 55 $m^{0.5}/s$ were assessed for the Chézy coefficient corresponding to measured flow discharge of 13'600 and 14'300 m^3/s respectively. When simulating significant changes in water level, as is the case of the simulated scenarios, different Chézy values were considered in order to account of flow resistance due to island and alluvial plane vegetation at left margin. Therefore the following exponential law was introduced to simulate the Chézy parameter, C, change with flow discharge, giving 55 and 38 $m^{0.5}/s$ for 15 and 3 m water depth, h, respectively.

$$C = 29.5 \cdot h^{0.23} . \qquad [1]$$

Figure 10 shows the depth maps at starting ending data (2040) as it results for last decade scenario and for the RCA projection with constant, equal to 55 $m^{0.5}/s$, and variable Chézy. The flow resistance due to vegetation reduced the upstream island erosion; this occurrence in some degree maintains the main channel morphology at upstream right reach and therefore reduces the activation of the secondary reach at the left margin. A further reduction of island erosion resulted by limiting the water level to floodplain level.

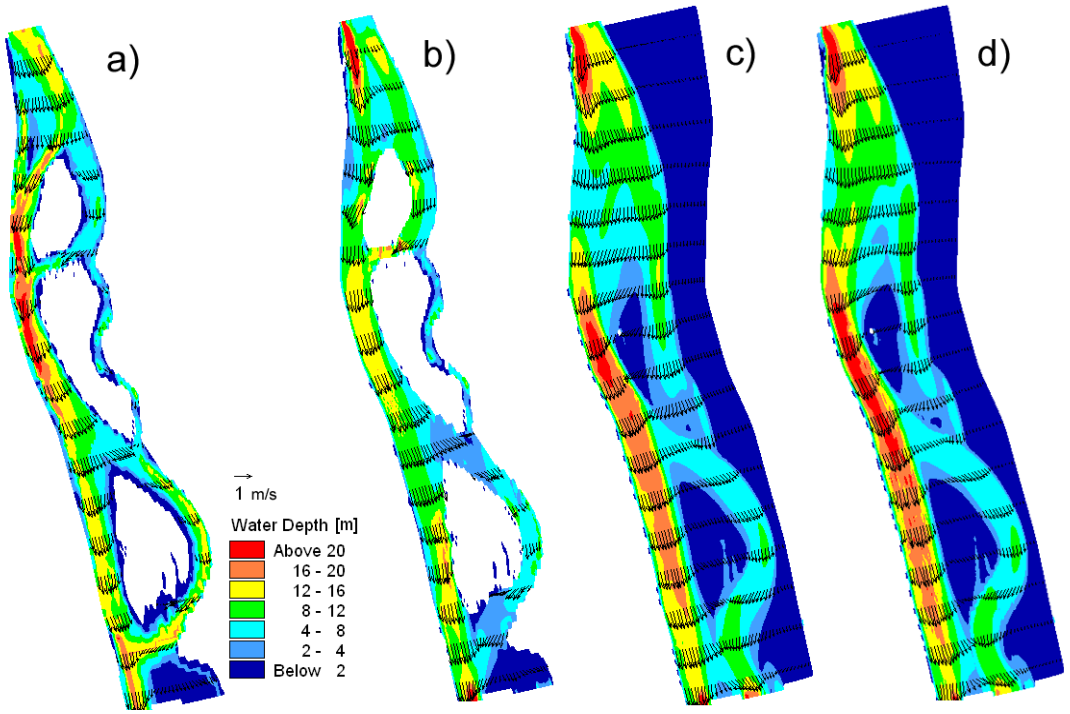

Figure 10. Initial and resulting water depth maps from 2D model simulations of 2010-2040 period for last decade (b), RCA (c) and RCA with variable Chézy (d) scenarios.

Sedimentation in navigation route

The study zone corresponds to 'Paso Borghi' (Figure 11), a critical stretch at the Lower Paraná River, where maintenance of the navigation channel is critical for the region economy.

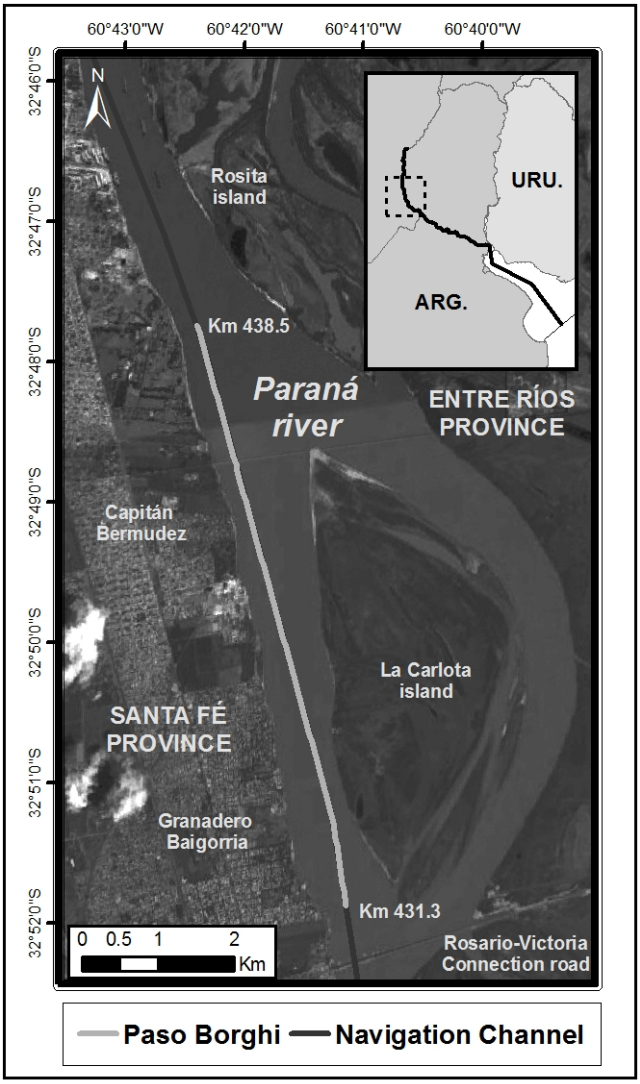

Figure 11 Paso Borghi location at Lower Parana River.

Sedimentation rates in Paso Borghi are calculated by AGRADA software (Menéndez, 1994), which simulates the sedimentation process in navigation channels driven by the action of currents (including

suspended and bed load transport and morphological evolution (Figure 12). AGRADA is based on a parametric hydrodynamic model and a transport model in the vertical plane at the flow direction (2D-V).

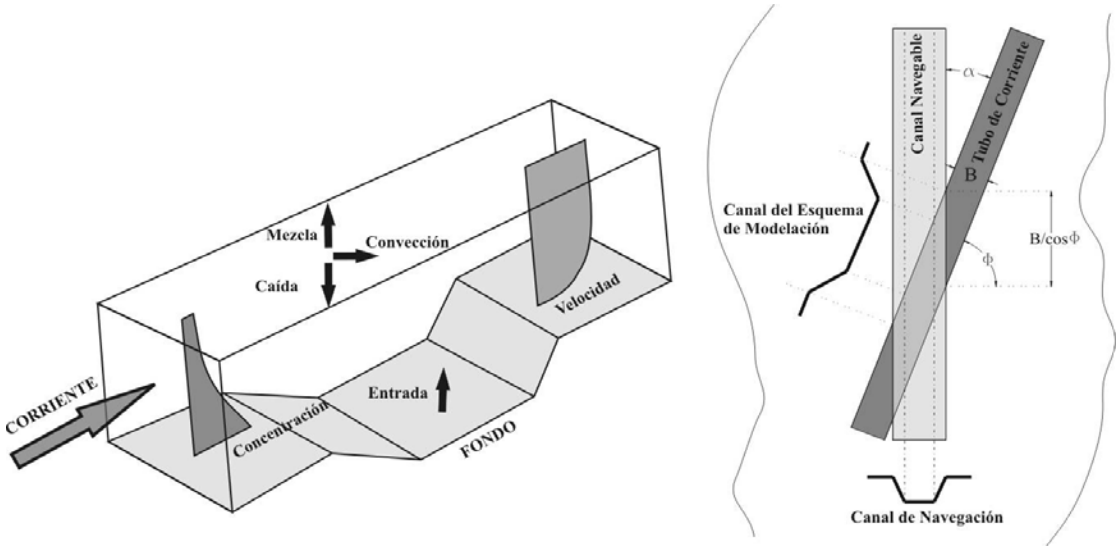

Figure 12 Navigation channel scheme by AGRADA software.

The hydrodynamic model solves vertical profiles for velocity components (horizontal and vertical), the bottom shear stress distribution and the vertical profile of the turbulent mixing coefficient. Since the bottom level variations due to the sedimentation process occurs on large time scales compared with the hydrodynamic scale, it is possible to assume that hydrodynamic conditions instantly adapt to these changes. The vertical profile of the horizontal component of velocity (axis x) is presented as a parametric family of functions, consisting of a logarithmic and a turbulent component (van Rijn, 1987):

$$u(x,z) = A_1(x) \cdot \ln\left(z/z_0\right) \cdot u_h(x) + A_2(x) \cdot F(\eta) \cdot u_h(x) \qquad [2]$$

where z is the vertical coordinate measured from the bottom, z_0 the height of the point where velocity is zero, u_h the surface velocity, A_1 and A_2 local parameters (independents from z), η the non-dimensional vertical coordinate (varies between 0 and 1 while z does between z_0 and the free surface), and $F(\eta) = 2\,\eta^{t} - \eta^{2t}$, being t another local parameter. The turbulent component is necessary because when there are abrupt changes in the bottom, as in this case where the current flows through a dredged navigation

channel, vertical velocity profile deviates from the equilibrium conditions. Known the horizontal component of velocity profile, the distribution of the vertical component *w* can be obtained numerically vertically integrating the equation of continuity. The bottom shear stress, meanwhile, is calculated by differentiating the velocity vertical profile. Another parametric distribution was applied for the turbulent mixing coefficient (van Rijn, 1987).

Crossing the channel, the streamlines have a refraction effect, which involves a change of direction (greater alignment with the channel) and width (narrowing), which implies a change in current intensity. This effect can be determined from abacuses that were obtained by numerical simulations (van Rijn, 1991).

The time scale associated with bed load transport is much smaller than the hydrodynamic one, so that transport can be seen instantly adjusts to local conditions. This means that it is necessary to develop an equation of time evolution of the bed load transport: it is only necessary a simple formula. However, since the velocity profile is not in equilibrium, it is desirable to apply a more general formula for transport that usually employed. The following equation, proposed for van Rijn (1987) was used for the solid discharge of non-cohesive sediment transported as bed load (Q_{sf}):

$$\frac{Q_{sf}}{b \cdot d_{50} \cdot \left(g \cdot d_{50}\right)^{1/2}} = 0.053 \cdot \sqrt{\Delta} \cdot D_*^{-0.3} \cdot T_m^{2.1} \qquad [3]$$

where d_{50} is the mean diameter of the particle, D_* the non-dimensional size of the particle, Δ the relative density, b the width of the control volume, g the acceleration due to gravity, and T_m the mean value of the state parameter.

Bed load transport over the banks of the navigation channel not strictly follow the direction of flow, since the action of gravity incorporates a component of the weight towards the center of the channel generating a deviation. The deviation angle is calculated based on a formula given by Fredsoe (1978), which depends on the inclination of the bank and the internal friction angle.

The suspended sediment transport model includes the longitudinal advection (in flow direction), the effective vertical advection and turbulent diffusion according to the vertical direction (van Rijn, 1987):

$$\frac{\partial(b\cdot u\cdot c)}{\partial x}+\frac{\partial\left(b\cdot(w-w_s)\cdot c\right)}{\partial z}=\frac{\partial}{\partial z}\left(b\cdot\varepsilon_s\cdot\frac{\partial c}{\partial z}\right) \qquad [4]$$

where c is the volumetric concentration of sediment, w_s the settling velocity of sediment and ε_s the turbulent mixing coefficient in the vertical direction. This equation is solved numerically using the finite element method with a mesh of quadrangular elements. As boundary condition at the bottom is common to assume a local equilibrium, considering that deposition equals resuspension. This assumption allows an equation for suspended sediment concentration at that point, resulting in a formula compatible with the treatment of van Rijn (1987) for bed load transport:

$$C_a=0.03\frac{d_{50}}{a}\frac{\overline{T_m^{1,5}}}{D_*^{0,3}} \qquad [5]$$

On the free surface is imposed a zero sediment flow, whereas in the entrance surface of the control volume it is considered a local equilibrium profile for concentration. Known concentration, suspended sediment discharge (Q_{ss}) is calculated numerically integrating the flow over the entire cross section.

The model for bottom level evolution is represented by the Exner Equation:

$$\frac{\partial\left(b\cdot z_f\right)}{\partial t}+\frac{1}{1-p}\cdot\frac{\partial Q_s}{\partial x}=0 \qquad [6]$$

where z_f is the bottom level, t the time coordinate, p the porosity, and $Q_{st} = Q_{sf} + Q_{ss}$ the total solid discharge. This equation is solved numerically using a finite difference method, providing, from the longitudinal distribution of the total solid discharge, the variation in the bottom level.

Basic information

Paso Borghi extends (for the actual depth of dredging) between km 431.3 and km 438.5 of the Paraná River navigation route (coordinates rises upstream). Bathymetric surveys data and estimated dredged

volumes from Paso Borghi for the period Apr-12-2008 –Apr-12-2009, provided by the *Organo de Control de Concesiones de Redragado y Señalización* which is under the *Dirección Naciona de Vías Navegables* (DNVN) of the national argentine government.

Figure 13 represents a scheme of the maintenance dredging operations carried out during the year of analysis, indicating dates and dredged volume. It can be seeing that the operations are concentrated in two streams: Lower Paso Borghi (km 431.3 – km 433.9) and Upper Paso Borghi (km 436.8 – km 438.5). Based on this data it was determined the mean annual sedimentation rate in each segment of 100m, obtaining the distribution of the Figure 14.

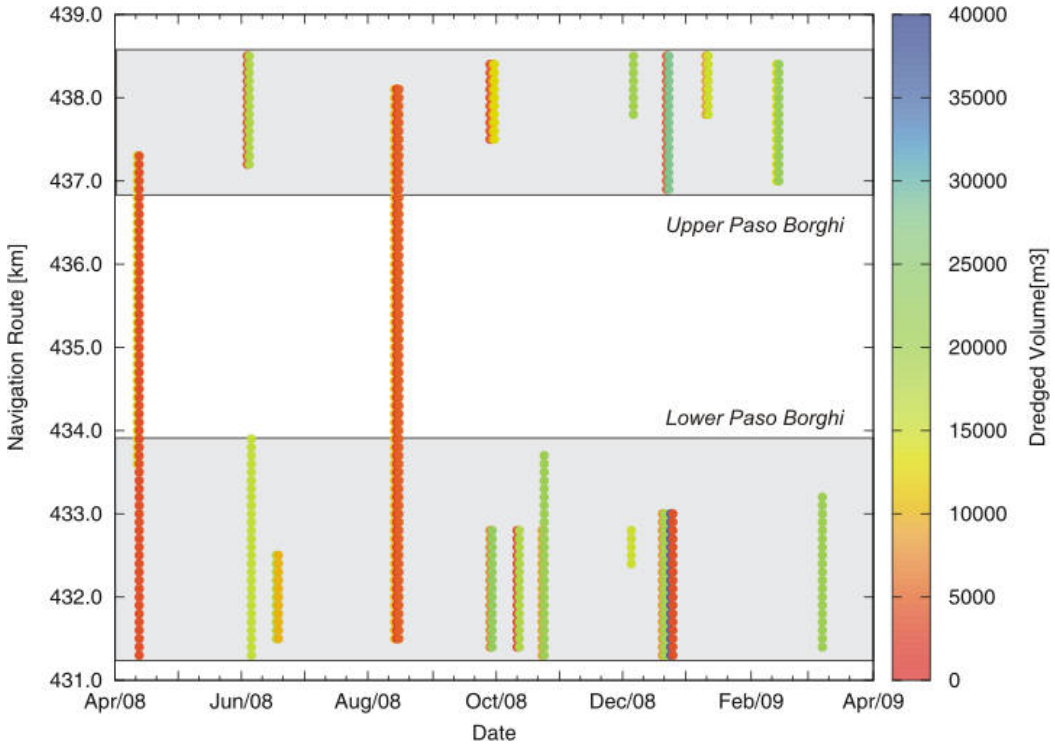

Figure 13 Dredged volumes, location and date of maintenance dredging operations.

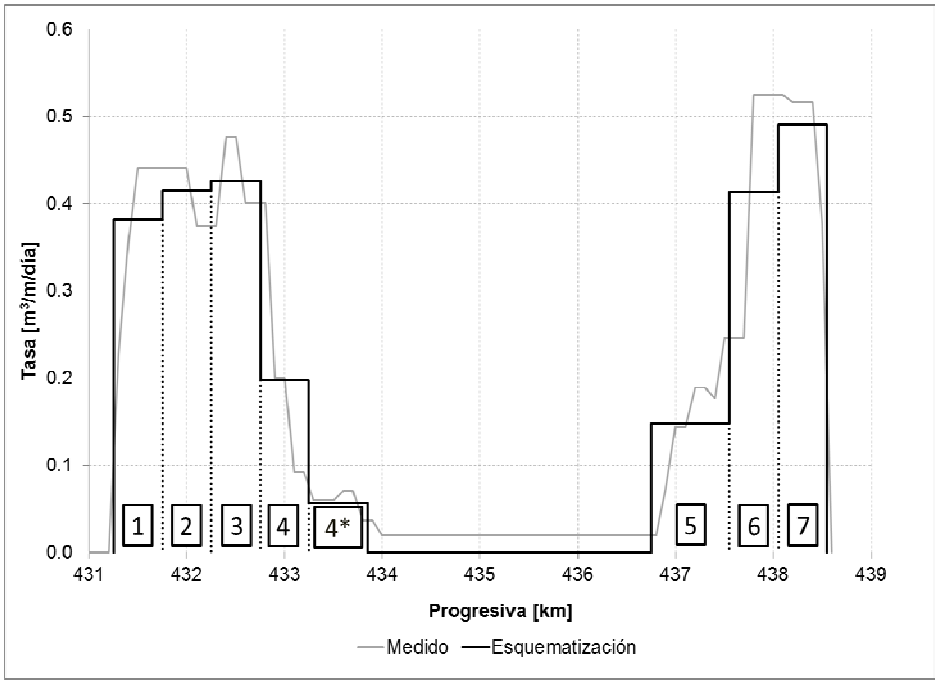

Figure 14 Schematic interpretations of the dredged volumes.

To simplify the analysis, each of both streams of Paso Borghi (Upper Paso Borghi and Lower Paso Borghi) was subdivided in sub-stretches, considering four for Lower Paso Borghi (Nº 1 to 4) (all with a length of 500 m, neglecting the contributions of the sub-stretch Nº 4*), and 3 sub-stretches (Nº 5 to 7) for Upper Paso Borghi (one with a length of 800 m and the other two of 500 m). In the same figure it is represented the mean dredged rate for each sub-stretch. Representative sedimentation rates for the modeling calibration were obtained assuming that the dredged volume is equal to the settled sediment volume.

Additionally, the time between dredging operations was calculates for each segment. Figure 15 shows the mean annual value for each segment of 100 m. It is observed that 40 days is a typical period between dredging operations for the whole Lower Paso Borghi; in the rest dominates a period around 60 days.

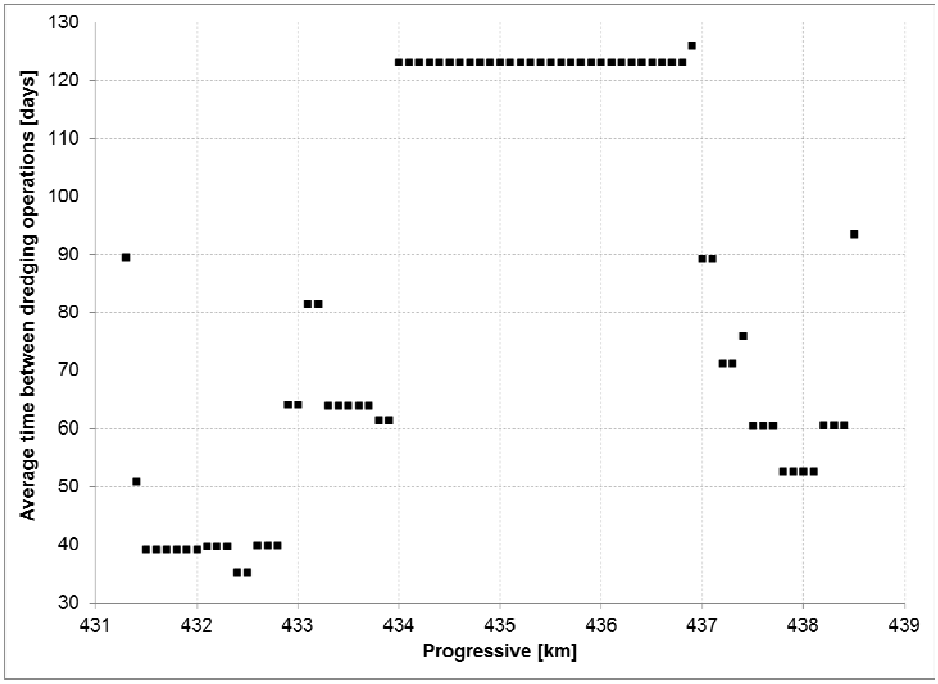

Figure 15 Average periodicity between dredging operations in 2008-2009 season at Paso Borghi.

A hydrodynamic model using HIDROBID II (a 2D-H software; Menéndez, 1990), was implemented in a domain extended from Km 452 of the navigation route to Rosario-Victoria Bridge, Km 430.0. With detailed bathymetric information available from an ad-hoc survey (Guerrero et *al.*, 2011), a Digital Terrain Model (DTM) for the river bottom with cells of 40 m x 40 m was developed.

For the calibration of the hydrodynamic model (2D-H), ADCP data from the UNIBO-FICH survey (June 29 to July 3, 2009) was used. This data was used too to impose an upstream boundary condition of 13'740 m^3/s. As a downstream boundary condition a water level was imposed (1.82 m over the local zero). For calibrating the model, Manning's roughness coefficient was adjusted (obtaining n = 0.025). Figure 16 shows a comparison between mean velocities from simulations and observations. Hydrodynamic parameters variables for 2D-V modeling (specific discharge; depth; and angle between the channel axis and the current line for each sub-model) from the 2D-H model.

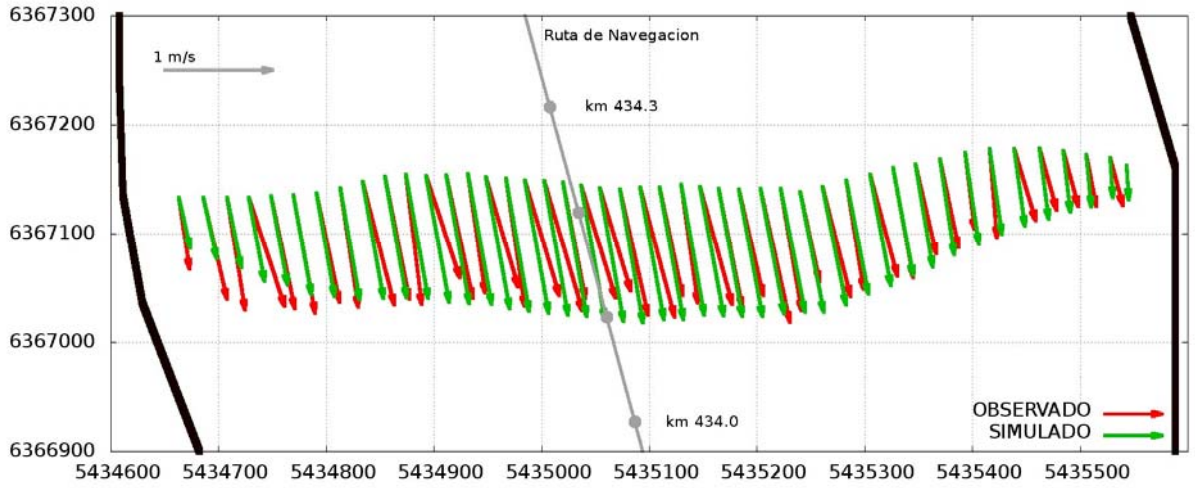

Figure 16 Velocity calibration in Lower Paso Borghi (observed values from UNIBO-FICH survey Jun/Jul 2009)

A sedimentological model was constructed for each sub-stretch. From data of periodical bathymetries of cross sections during the studying period, a representative profile for each one was schematized as the navigation channel (bottom width of 116 m and banks with a rate 1V:5H, as indicated by the navigation authority) and horizontal bank plains at each side (Figure 17).

It is observed that there is no clear identification of the dredged channel in the profiles surveyed. Then, we established the following criteria: as a depth for the bank plain, a level corresponding to approximately the upper third of the measured levels, was taken to each side of the channel, while as a bottom elevation was selected a representative level of the lower third the measured levels.

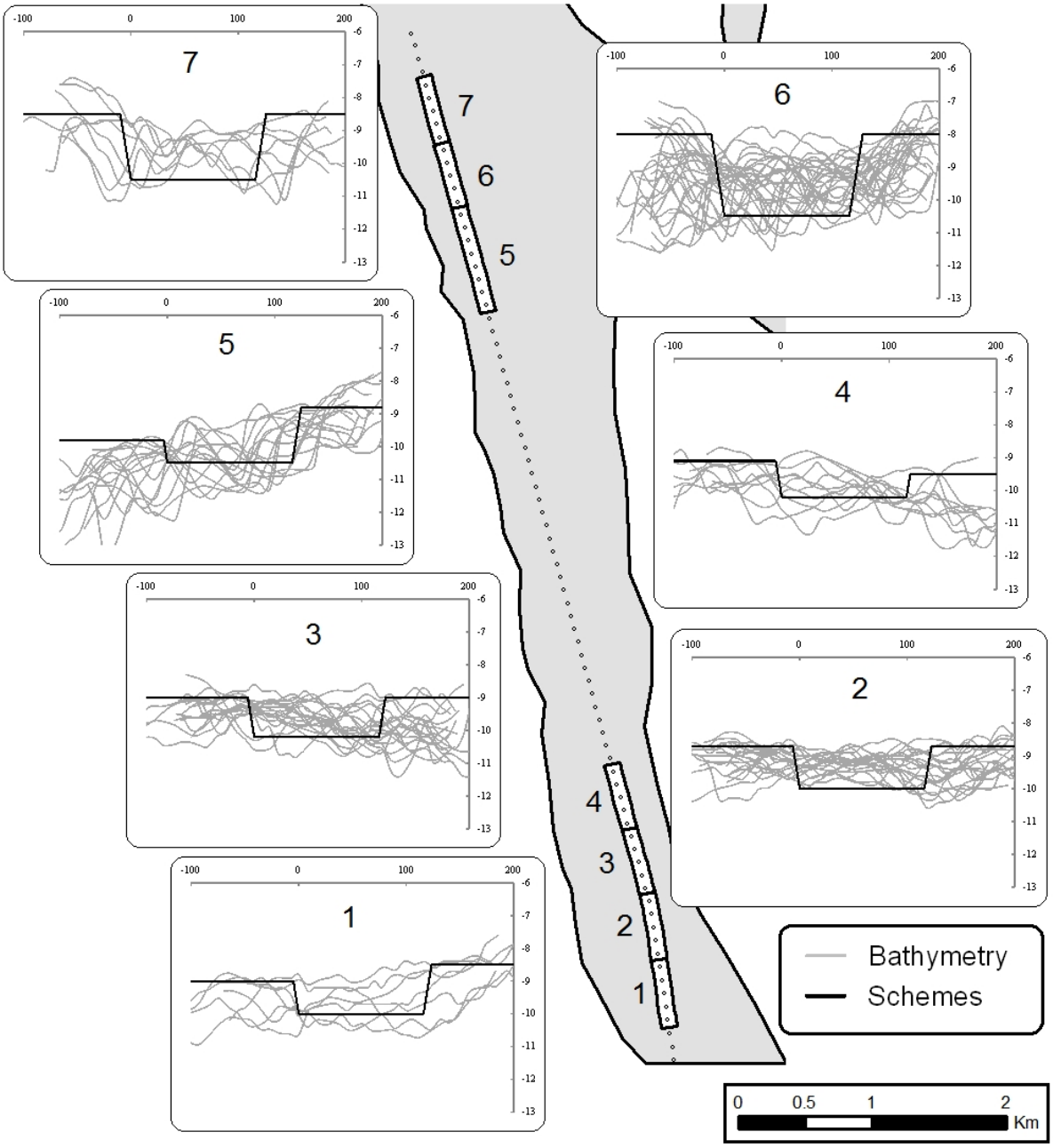

Figure 17 Dredged cross sections schematizations.

For all models a vertical discretization of 25 cells was adopted, with heights distributed logarithmically in order to have a higher resolution near the bottom. The domain begins 100 m upstream of the contour of the channel and extends to 300 m downstream of the other contour.

To calculate the average annual sedimentation in the navigation channel on the period of study (April 12th, 2008 - April 12th, 2009) the mean annual liquid discharge was used (13'100 m^3/s). Based on results

of the 2D-H hydrodynamic model, stream tubes of 250 m^3/s were constructed (Figure 18). For each sub-stretch, one stream tube was selected as representative to provide the conditions of incidence to the control volume model of sedimentation (width, water level and orientation of the flow velocity relative to the axis of the subsection) for running the 2D –V hydrodynamic model (Table 1).

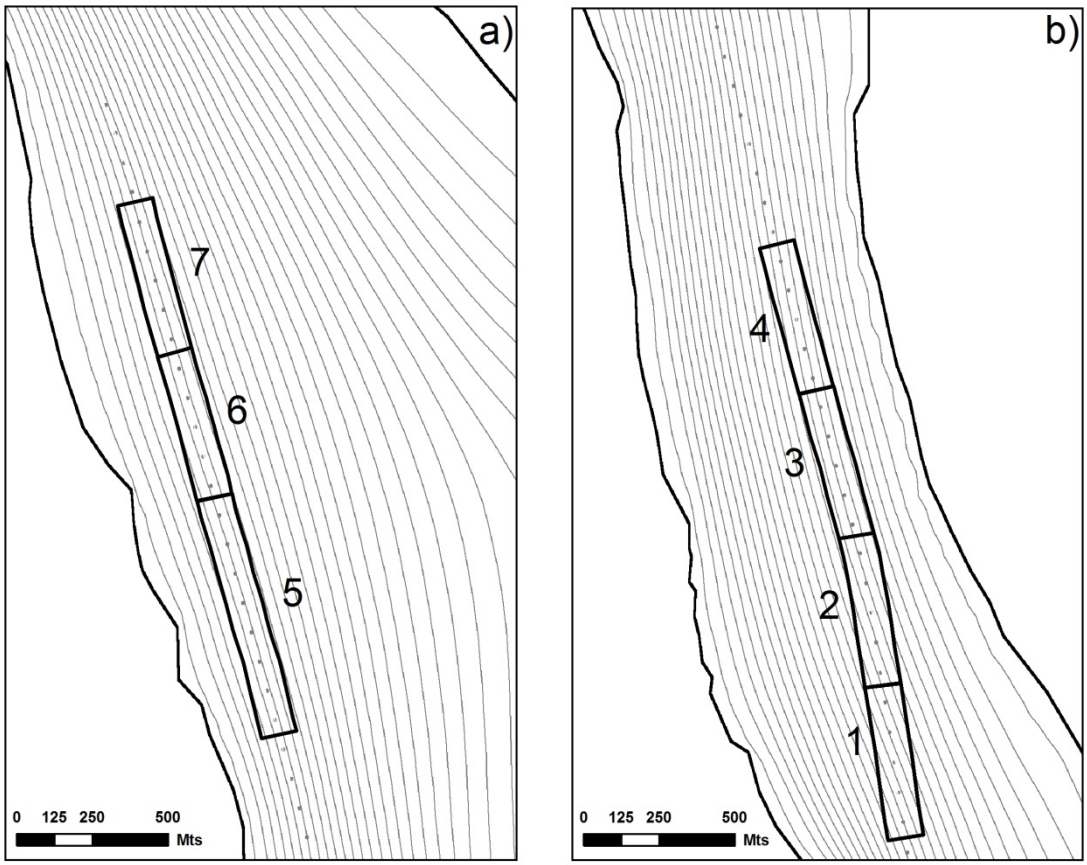

Figure 18. Tubos de flujo para caudal medio en a) Borghi Superior y b) Borghi Inferior. Por claridad sólo se grafican los tubos cada 500 m^3/s.

Table 2. Values of incidence for the hydrodynamics parameters.

Nº	Sub-stretch (km)	$Q_{specific}$ (m3/m/s)	Level from local zero (m)	Angle (º)
1	431.25-431.75	12.4	2.507	11.6
2	431.75-432.25	12.3	2.515	5.0
3	432.25-432.75	13.0	2.528	0.0
4	432.75-433.25	13.4	2.541	4.3
5	436.75-437.55	12.4	2.658	1.8
6	437.55-438.05	11.1	2.680	2.0
7	438.05-438.55	11.9	2.687	1.0

Based on available data along the navigation route (Menendez, 2002), a mean grain diameter (d_{50}) for the bottom sediment was determined: 260 μm. Settling velocity was calculated by van Rijn (1987) formulation and is 3.7 cm/s. The porosity of the sand was defined as 0.4. It was verified that the suspended sediment concentration profile modeled at the bank plain is consistent with measures 30 kilometers downstream Paso Borghi, at Km 406.5 (Royal Boskalis and Ballast Ham Dredging, 1992). Figure 19 illustrates the comparison for all sub-stretches.

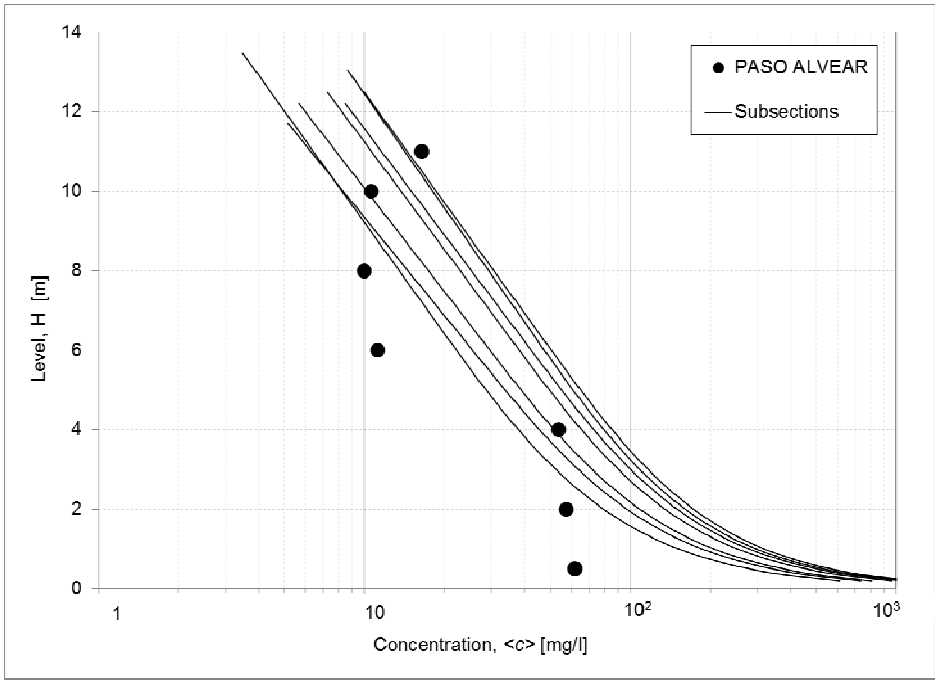

Figure 19. Vertical profile of concentration.

Table 3 shows mean vertical concentrations, <*c*>; suspended load, bed load, total load and the ratio between suspended and bed load for each sub-stretch. Mean concentrations are consistent with those measures at the region (Guerrero et *al.*, 2011). Therefore, it is observed that suspended load - bed load ratio is in the order of 7, consistent with available measurements (Szupiany et *al.*, 2010).

Table 3. Sediment load for each sub-stretch.

Nº	<c> (mg/l)	Qss (mg/m/s)	Qsf (mg/m/s)	Qst (mg/m/s)	Qss/Qss
1	69.5	889	126	1015	7.0
2	78.2	1004	142	1147	7.1
3	88.6	1212	167	1379	7.2
4	80.4	1298	177	1475	7.3
5	39.1	471	67	538	7.0
6	52.4	577	86	663	6.7
7	56.9	672	98	770	6.9

The sediment transport process means that, when currents cross the navigation channel, there is an advance of sedimentation at the upstream bank and a retreat by erosion of the downstream bank, which is called *'trap effect'*. In addition, the action of gravity on the transport over the banks generates a diffusion effect, which is called '*gravitational effect*'. For simplicity, these two effects were calculated separately. The representative angle of refraction corresponds to the midpoint of each bank to calculate the effect trap, and the deflection angle corresponds to the same points to calculate the gravitational effect. Figure 20 shows the evolution of the cross section in one sub-stretch with each effect.

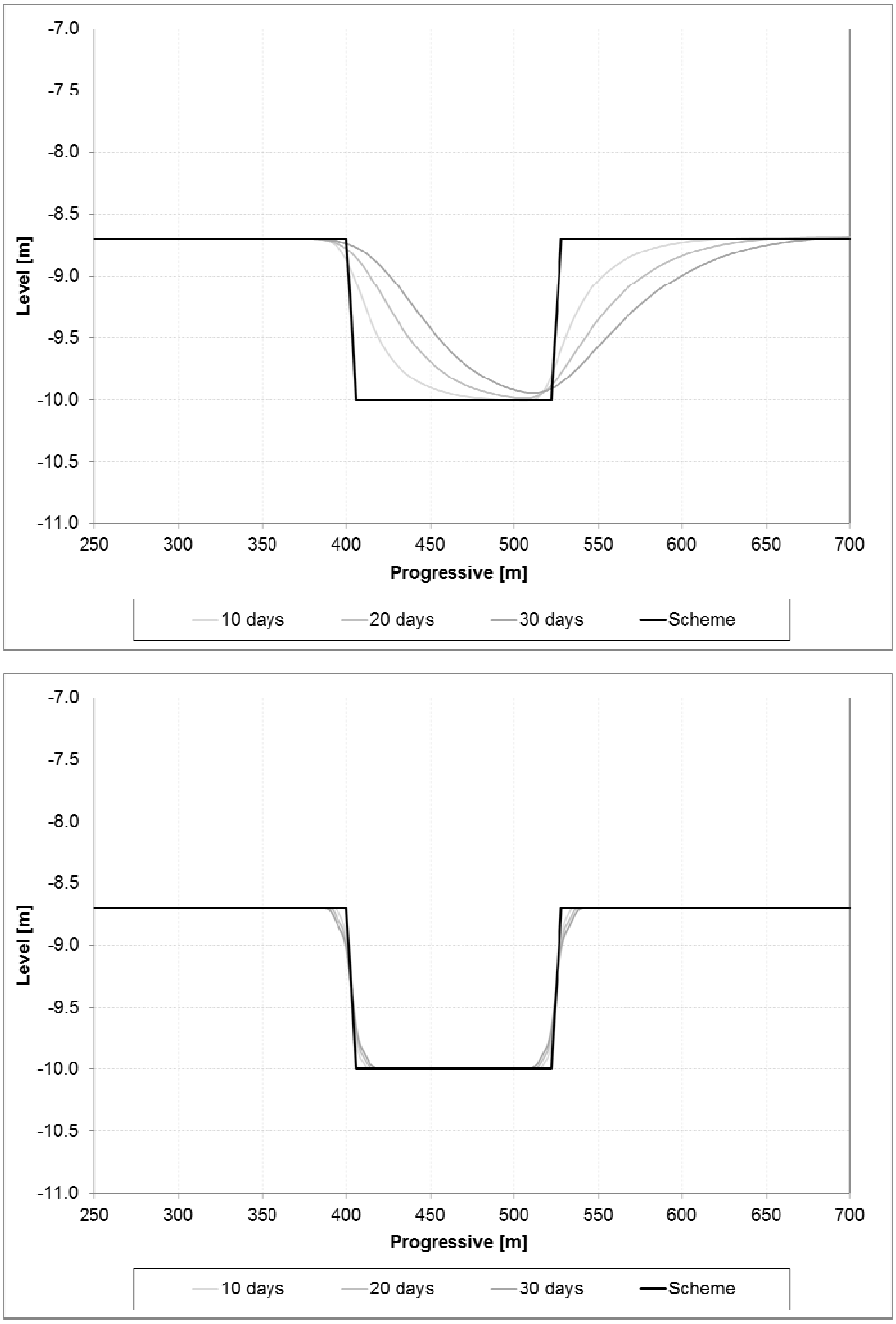

Figura 20. Cross section evolution (sub-stretch Nº 2): a) *trap effect;* b) *gravitational effect*

From the results for 1 month since the dredging (representative time scale between maintenance dredging), were determined sedimentation rates per unit length for each sub-stretch. The difference between the bottom levels at the end and at the beginning of the simulation and the integration between

contours was made to calculate the sedimentation rates. For some subsections this rate was recalculated using a time of 2 months, showing little sensitivity.

The agreement between the sedimentation rates calculated for each sub-stretch versus data from maintenance dredging was satisfactory (which is a validation of the calculation methodology), except for the first sub-stretch where the calculated value was excessive. For this sub-stretch the incidence angle was reduced as a calibration process. Figure 21 shows final results.

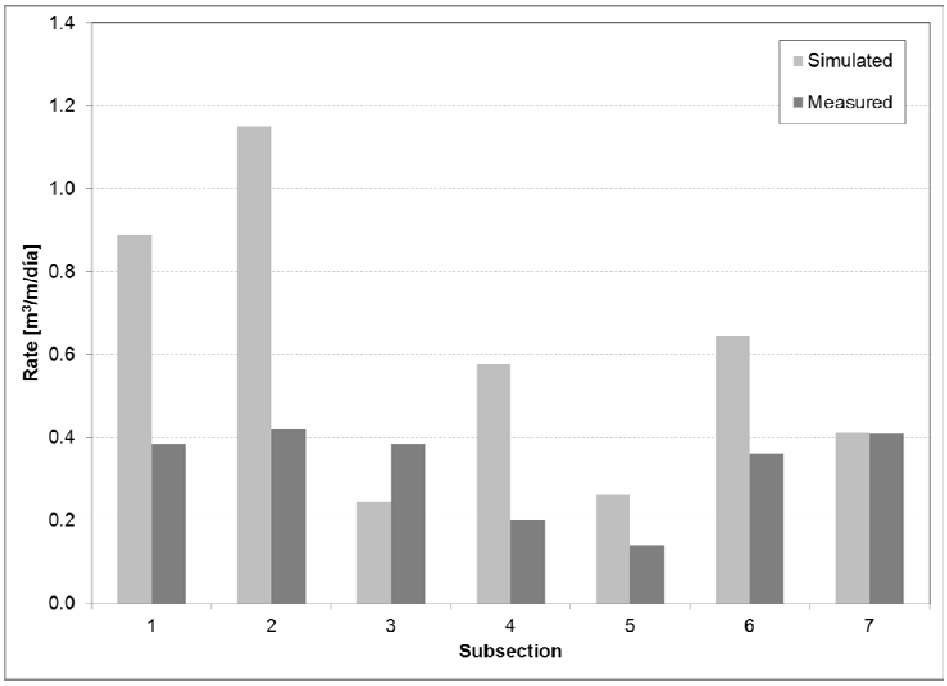

Figura 21. Sedimentation rates (per length unit) calculated and from data of dredging.

Future scenarios

To better understand system impacts, we have proceeded to consider potential positive or negative changes in discharges as future scenarios. A baseline scenario (average of the period 1994-2010) was taken as a present scenario. For all these scenarios it was assumed that the morphology of the Parana River is not affected by the change in discharges, no changes on bottom levels outside the dredging area (*bank plains*). Strictly this is not true, since there is a historic morphological evolution in the area over

decadal time scales (Castro et al., 2007), which also would be influenced by the discharge change (the assessment of this effect is not in the aim of this work).

First, scenarios under the hypothesis of maintaining the current levels of dredging were tested (despite the change of mean discharge, the reference level required for navigation does not change). This would represent a situation in which the managing authority of navigation does not assume the hydrological change. The results (presented in Figure 22) shows that the settling volume increases with increasing discharges and vice versa. The relative rate of variation of the settled volume is significantly greater than the flow (in absolute value).

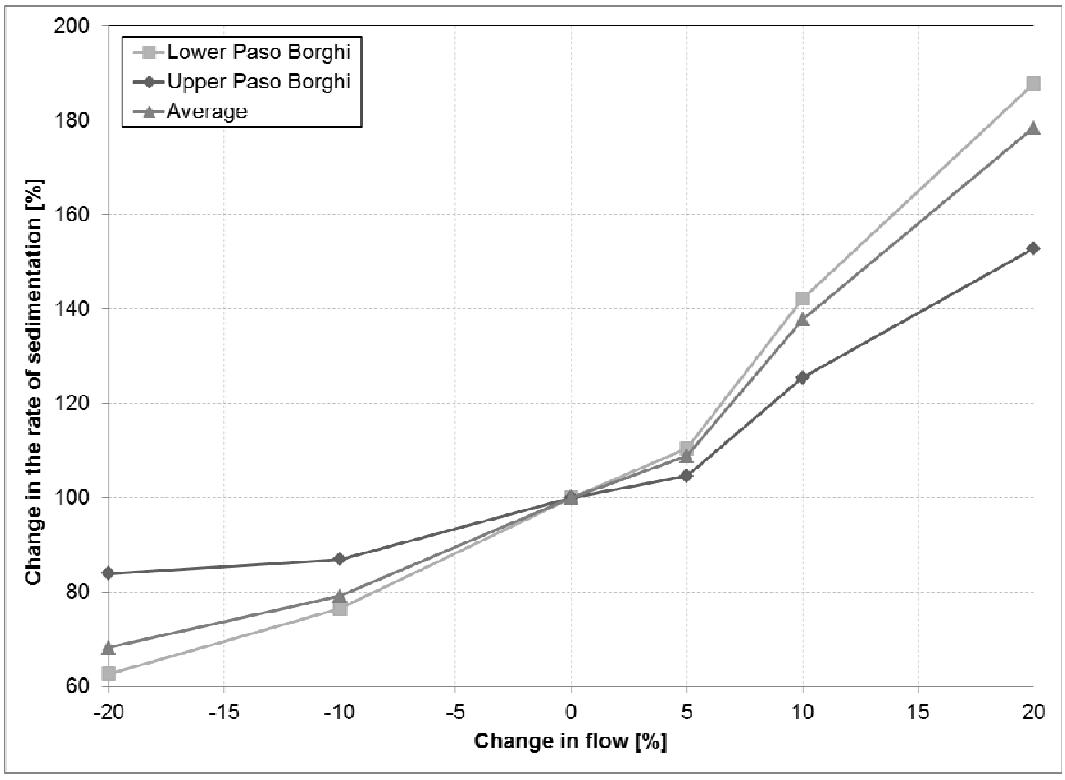

Figura 22. Change in sedimentation rates with the same dredging level.

Second, we considered scenarios in which the dredging depth was adjusted to reflect the change in the reference level required for navigation, taking in account the change in the mean discharge (it would be the case in which the managing authority observed the hydrological change). It was assumed that the

reference level varies in the same amount as the water level associated with the mean discharge. The results are presented in Figure 23, where it is observed that now the trend is the opposite. The settled volume increases when the mean discharge rate decreases (and vice versa) because the decrease in depth forces an increase in the depth of the navigation channel causing more sedimentation. The relative rate of change of sedimentation is only moderately higher than the discharge rate (in absolute value). For increases greater than 10% of the mean flow would not be necessary to carry out dredging in some sub-stretches.

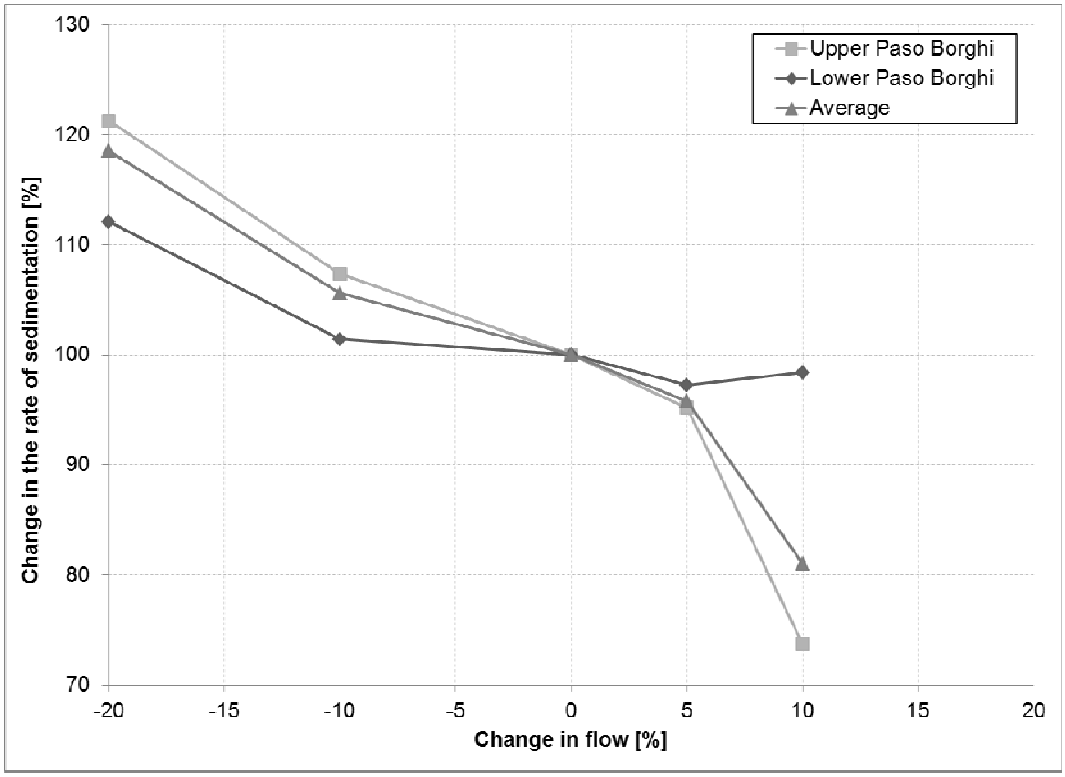

Figure 23. Change in sedimentation rates fitting the reference level for dredging.

Results

Results of numerical simulations of future scenarios (hydrological projections) that would impact on the navigation route 'Santa Fe to the Ocean' at the Parana River were presented.

The 2D simulated reach of Lower Paraná is only 24 km long, but includes two bifurcations and two junctions at the San Martin-Rosario area and therefore it significantly represents divagation of the river channel that interferes with the navigation way. The 1D numerical simulation of two future scenarios substantiate the observed stability of river longitudinal slope during the XX century, the past morphological changes being related to thalweg planimetric divagation, island formation-erosion and braiding-meandering tendencies. In such dynamic-equilibrium of sediment transport along the river, the climate projections give rise to significant changes of river channel planimetric morphology that are related to the forecasted enhanced hydrology and to the consequent increase of water depth, flow and sediment discharges. The 2D model forced with such values simulates a significant increase of the sediment-hydraulic conductivities by means of secondary reach activation and the merging of meandering-bifurcated reaches. In particular, the simulated islands erosion that widens the active channel appears critical for the navigation way because it would gives rise to lower water depths notwithstanding the flow discharge increase. This process was partially reduced by simulating floodplain and island resistance to flow due to vegetation and the accretion of floodplain level due to fine sediment deposition during floods. Therefore the balance between floodplain accretion plus vegetation growth and sand transport within active channel is critical in determining the actual thalweg divagation.

Hydrological changes arising as a result of Climate Change will manifest themselves in changes in the rate of sedimentation in navigation channels, indicative of maintenance dredging needed to keep them operative. To quantify the effects of hydrological changes, it was necessary to implement a methodology for calculating the sedimentation by numerical modeling. To better understand the system dynamics,

positive and negative potential changes in discharges were considered as possible future scenarios. It was assumed that the morphology of the river is not affected by the change in discharges. The results of projections show that the change rate of sedimentation is, in absolute value, always greater than the flow. Specifically, if the current levels of dredging are maintained (no adaptation to hydrological changing), the settling volume would increase with increasing discharge rate and vice versa. If the levels of dredging are adjusted in order to adapt to a hydrological change, the trend would be opposite: the settling volume grew when the mean discharge rate of change decreases (and vice versa).

References

Amsler, M.L., Ramonell, C.G. y Toniolo, H., 2005. Morphologic changes in the Paraná River channel (Argentina) in the light of the climate variability during the 20th century, Geomorphology 70: 257-278.

Doyle M.E., Barros V.R., 2010. "Attribution of the river flow growth in the Plata Basin", International Journal of Climatology, DOI: 10.1002/joc.2228.

Castro, S. L., Cafaro, E. D., Gallego, M. G., Ravelli A. M., Alarcón J. J., Ramonell, C. G. y Amsler, M. L., 2007.Evolución morfológica histórica del cauce del río Paraná en torno a Rosario (km 456 – 406), CONAGUA 2007, Argentina.

De Wit, M. J. M., Van den Hurk, B., Warmerdam, P.M.M., Torfs, P.J.J.F., Roulin, E., Van Deursen, W.P.A., 2007. Impact of climate change on low-flows in the river Meuse. Climatic Change, Vol. 82, Núm. 3–4, pp. 351–372.

DHI Water & Environment, 2002. Mike21C River Hydrodynamics and Morphology, DHI, Horsholm, Denmark.

Fernandes C., Guerrero, M. & Barros, V., 2011, CLARIS LPB WP9: Water resources in La Plata Basin in the context of climate change. CLIVAR Exchanges Special Issues on LPB, No. 57, Vol. 16-3, 31-35, Indigo Press, Southampton, UK.

Fredsoe, J. Sedimentation of River Navigation Channels, ASCE, February, 1978, pp. 223-236.

Garcia N.O. and W.M. Vargas, 1998. The temporal climatic variability of runoff and precipitation in the Rio de la Plata basin. Hydrological Sciences Journal, 41 (3), 279-299.

Garcia N.O., Vargas W. M., Venencio M., 2002. About of the 1970/71 climatic jump on the Rio de la Plata basin. Proceedings 16th Conference on Hydrology. American Meteorological Society, pp. 138-141.

Guerrero, M., Szupiany, R.N., Amsler, M.L., 2011. Comparison of acoustic backscattering techniques for suspended sediments investigation, Flow Measurement and Instrumentation, 22, pp. 392–401.

Guerrero M., Di Federico V., Lamberti A. Improved calibration of a 2-D numerical model of Po River morphodynamics using MBES and ADCP measurements, J. Hydroinform., under review-a.

Guerrero M., Gaeta M.G., Lamberti A. Bed-roughness investigation for a 2-D model calibration: the San Martìn case study at Lower Paraná, Int. J. Sediment Res., under review-b.

Hawkes, P.J., Pauli, G., Moser, H., Arntsen, Ø.A., Gaufres, P., Mai, S., White, K. Impacts of climate change on waterborne transport, Civil Engineering, 163, 2010, pp. 55-63.

Jaime, P.R. and Menéndez, A.N., 2002. Análisis del régimen hidrológico de los ríos Paraná y Uruguay, Informe LHA-01-216-02, INA, Ezeiza, Argentina.

Maciel, F., Díaz, A., Terra, R., 2010. "Variabilidad multi-anual de caudales en ríos de La Cuenca del Plata", IAHR-AIIH, XXIV Congreso Latino Americano de hidráulica, Punta del Este, Uruguay, November.

Menéndez, A.N., 1990. Sistema HIDROBID II para simular corrientes en cuencos, Revista Internacional de Métodos Numéricos para Cálculo y Diseño en Ingeniería, 6 (1), pp. 25-36.

Menéndez, A.N., 1994. Simulación numérica de la sedimentación en canales de navegación, Información Tecnológica - Revista Latinoamericana, 5 (4).

Menéndez, A.N., 2002. A Methodology to Scale Turbidity Plumes, 2nd Int. Conf. New Trends in Water and Environmental Engineering for Safety and Life: Eco-compatible Solutions for Aquatic Environments, Capri, Italy, Junio.

Millerd, F. The potential impact of climate change on Great Lakes international shipping. Climatic Change, Vol. 104, 2011, pp. 629–652.

PIANC (World Association for Waterborne Transport Infrastructure), 2008. Waterborne Transport, Ports and Waterways: A Review of Climate Change Drivers, Impacts, Responses and Mitigation, report of PIANC EnviCom Task Group 3, Climate change and navigation, Brussels, Belgium.

Royal Boskalis and Ballast Ham Dredging, Ruta de Navegación de Ultramar San Martín – Océano, Informe para la Licitación del Dragado de la Vía Navegable, Dirección de Vías Navegables, Argentina, 1992.

Solman, S., Sanchez, E., Samuelson, P., Berbery, E. H., Recca-Remedio, A., Porfirio da Rocha, R., Chou S. & Li, L., 2011, CLARIS LPB WP5: Regional Climate Change assessments for La Plata Basin. CLIVAR Exchanges Special Issues on LPB, No. 57, Vol. 16-3, 19-21, Indigo Press, Southampton, UK.

Sung, R.Y.J., Burn, D.H., Soulis, E.D, 2006. A Case Study of Climate Change Impacts on Navigation on the Mackenzie River, Canadian Water Resources Journal, Vol. 31, Núm. 1, pp. 57-68.

Szupiany, R., Hernandez, J., Amsler, M., Fornari, E., Parsons, D., Best, J.L., Trento, A., 2010. Comportamiento hidro-sedimentológico en bifurcaciones de un gran río, XXIV Congreso Latinoamericano de hidráulica, Punta del Este, Uruguay, Noviembre.

U.S. Army Corps of Engineers, 2008. HEC-RAS River Analysis System, Hydraulic Reference Manual.

Van Rijn, L.C.J., 1987. Mathematical modelling of morphological processes in the case of suspended sediment transport, Delft Hydraulic Communication 382.

Van Rijn, L.C.J., 1991.Sedimentation of dredged channels and trenches, In Handbook of Coastal and ocean Engineering, John B. Herbich Editor, Cap. 9, Vol. 2, pp. 615-618.